

TECHNICAL REPORT

Development of In-vessel Type Control Rod Drive Mechanism for Marine Reactor

Toshihisa ISHIDA^{1,*}, Shou IMAYOSHI², Tsutomu YORITSUNE¹, Hiroshi NUNOKAWA¹,
Masa-aki OCHIAI¹ and Yuichi ISHIZAKA^{3,†}

¹Department of Nuclear Energy System, Japan Atomic Energy Research Institute, Tokai-mura, Naka-gun, Ibaraki 319-1195

²Visiting Researcher in Japan Atomic Energy Research Institute

³Once cooperative staff of Japan Atomic Energy Research Institute

(Received February 8, 2001)

A highly reliable control rod drive mechanism (CRDM) installed inside the reactor vessel has developed for use of an advanced marine reactor. This CRDM contributes to compactness and simplicity of the reactor system, and it can eliminate the possibility of a rod ejection accident. The CRDM works in the high temperature and high pressure water—310°C and 12 MPa, the same atmosphere as the primary loop. Driving force is produced by a synchronous motor with the rotor of a permanent magnet, which has been developed. An innovative latch mechanism using separable ball nuts can latch the driving shaft connecting the control rod and de-latch it for scram. The rod position detector using a magnetostrictive wire type sensor on the principle of Wiedeman effect has been developed, accuracy of which is verified to have a detecting error within 1.2 mm. Ball bearings for thrust and radial supports in rotation have been developed to be capable of working under the high temperature water for a long period. Under condition of high temperature water, the performance tests on latching, de-latching, holding and vertical movement, and durability test were conducted to verify the design conditions. This CRDM can be applied to not only the marine reactor, but also to light water reactors, PWR and BWR.

KEYWORDS: control rods, control rod drive mechanism, in-vessel type CRDM, electric motor driven type, marine reactors, latch mechanism, ball bearing operation, high temperature water

I. Introduction

Nuclear power is one of promising power source for ship propulsion. Japan Atomic Energy Research Institute (JAERI) has studied the design of an advanced marine reactor, MRX,¹ with thermal output of 100 MW for the main use of nuclear-powered ship. In general, the reactor power of large scaled pressurized water reactor (PWR) for electricity generation is controlled by a chemical shim and/or control rods in the normal operation. A marine reactor, however, adopts the reactor control system using only the control rods, since rapid response of the reactor power is required for heavy and frequent load change due to change of ship propulsion, and a complex chemical processing system to deal the soluble boron is avoided.

Most of the control rod drive mechanisms (CRDMs) used in the PWRs are attached outside of the reactor vessel, and their shafts connecting with the control rods are covered with the pressure housings. A rod ejection accident (REA) or a loss of coolant accident (LOCA) caused by rupture of the pressure housing are required to postulate its occurrence in the safety evaluation corresponding to the Japanese governmental “PWR licensing safety review guideline.” These postulated accidents in large scaled PWRs, however, do not always give a severe impact, since these accidents are mitigated by adoption of great many CRDMs and the chemical shim, *i.e.*, the reactivity of control rod cluster operated by one CRDM are relatively small.

On the contrary, the reactivity of the control rod cluster of the marine reactor is inevitable to become a large value, because it has to be large enough to maintain a sub-criticality of the reactor in a cold state even under condition of an one-rod stuck, stated in the provision of IMO (International Maritime Organization) provided for the nuclear merchant ships. This leads to that the REA may result in very severe accidents for the marine reactor if it adopts the same type CRDMs as large scaled PWRs.

In the design of MRX, an in-vessel type control rod drive mechanism (INV-CRDM) is adopted to cope with this difficulty: The whole of the control rod drive mechanism is installed inside the reactor pressure vessel. It is natural to consider that the possibility of these accidents can be eliminated for the INV-CRDM as long as the reactor pressure vessel is intact. Adoption of the INV-CRDM can also contribute to compactness of not only the reactor vessel but also the containment vessel by using effectively the upper space inside the reactor vessel, and to simplicity by eliminating the cooling system of CRDM. Compactness and simplicity of the reactor system are ones of design targets especially in marine reactor design.

There are two types of the INV-CRDM concerning the driving force—driven by a hydraulic force and by a driving motor. The former is driven by the hydraulic force which is produced by pumps outside of the reactor vessel and transmitted through a pipe penetrating the reactor vessel. The latter is driven by an electric motor. In general, the former needs a rather complicated piping system including pumps, valves, pipes *etc.*, while the latter does not. Furthermore, the latter can easily attain a fine adjusting and control rapidly the position of control rods. For the latter, however, there are sev-

*Corresponding author, Tel. +81-29-282-6368, Fax. +81-29-282-6367, E-mail: ishida@koala.tokai.jaeri.go.jp

†Present address: Chuou-chou, Kume-gun, Okayama 709-3705.

eral technical subjects to be developed, since it works in the primary water, the high temperature and high pressure water. The former INV-CRDMs are adopted in Chinese NHR^{2,3)} for heat supply.

The MRX was designed to adopt the in-vessel type and motor-driven INV-CRDM considering that the reactor should respond to a heavy and rapid load change with a highly reliable, accurate, and simple control system. Basic design concept of the INV-CRDM of MRX was created in 1990. Main issues to be developed were designing of very compact INV-CRDM to be set in the narrow space inside MRX's reactor vessel, and to confirm reliable function of components such as the driving motor and the bearings under the severe condition. The original design and some of R&D were described in the interim report.⁴⁾ On the base of the original design, the final design with several improvements has completed recently, and its function was verified by tests with the full sized test assembly under condition of the high temperature and pressure water the same as that of MRX.

The present paper describes the final design and the performance test of the motor-driven INV-CRDM developed for the marine reactor.

II. Design Conditions

Design conditions of the INV-CRDM for the MRX are set up as follows, taking into account of being installed in a marine reactor.

(1) Compactness

The MRX adopts 13 sets of the INV-CRDM inside the core barrel. A cross-sectional size of each CRDM should be no more than 200 mm of a diameter, and the total length less than 2 m containing no spring, with the total stroke of 1,400 mm.

(2) Driving Function

The position of control rod connecting with the driving shaft should be controlled stably, smoothly and accurately in the normal operation. The speed of the driving shaft of movement upward and downward direction should be 0–300 mm per min except scram.

(3) Scramming Time

The MRX requires a short scramming time below 1.4 s, which counts from occurrence of a scram signal to complete insertion of the control rod into the core. Since a time for the control rod passing throughout the core is estimated as one second and a time delay of signal 0.2 s, a time for the INV-CRDM releasing the control rod after receiving the scram signal, called as a de-latch time, should be less than 0.2 s.

(4) Effect of Ship Posture

Ship posture due to a ship accident such as founder should be taken into account for function of a marine CRDM. For the MRX, the total scramming time is required less than 5 s in the event of inclination of 90° and the de-latch time less than 0.5 s. Even for an overturn, 180°, the scram should be securely completed.

(5) Circumstance for INV-CRDM Working

The INV-CRDM should be operated in the high pressure—12 MPa—and high temperature—310°C—water, since it works in the primary loop water. Components of the INV-CRDM such as the motor, the ball bearings *etc.*, are main

subjects to be developed. The INV-CRDM will be exposed by radioactive rays such as γ -ray and neutron. Effect of the radioactive rays on the materials should be clarified and a measure should be made, if necessary.

(6) Lifetime for Exchange of the INV-CRDM

The design of MRX requires the INV-CRDM to have lifetime of 20 years without exchange, and to be capable of scrambling at least 1,000 times in the lifetime.

III. Concepts and Design

1. Concept of the Whole Structure

A conceptual drawing of the INV-CRDM is given in **Fig. 1**. It consists of a driven motor, a latch mechanism, ball bearings, a driving shaft, a position detector, and so forth. Main functions of the CRDM are to move the control rods vertically upward or downward, and to insert them instantly into the core for scram.

Rotational torque generated by the driving motor should be transferred to the linear movement of the driving shaft. A mechanism to disconnect the driven motor from the driven shaft is necessary for a shorter scramming time. An innovative latch mechanism using separable ball nuts divided into three sections, which will be described later in Sec. III-3, has been developed to comply with these requirements simultaneously. A principle of the motion is illustrated in **Fig. 2**. In the normal operation, the driving shaft can move up and down by rotation of the driving motor when the separable ball-nuts of the latch mechanism are closed to grasp the driving shaft by energizing a latch magnet. In the scram, the separable ball-nuts will open to separate the driving shaft by de-energizing the latch magnet, and the driving shaft drops rapidly by the self-weight and spring force. Reliability of these motions at the severe condition should be certified and verified through functional and durability tests.

A built-in type synchronous motor with a permanent magnet for the rotor is applied to the driving motor, from viewpoints of compactness and simplicity. The permanent magnet should have an adequate remanence characteristics to operate under the condition of high temperature and for a long life-period, and also be of a high Curie temperature. Since the data on these characteristics were not published, main issue on the driving motor is firstly to obtain experimentally the reliable data on the permanent magnet.

Ball bearings are used for supporting the vertical load of most weights and a spring force, and the radial load of the rotational components. These bearings should be capable of working under the severe condition for the long lifetime, material of which was one of key issues to be developed.

The rod position detector is designed using a magnetostrictive wire type sensor on the principle of Wiedeman effect,⁵⁾ the first trial of application to a Light Water Reactor. This type sensor was prepared once in a experimental reactor of US FBR, CRBRP, but it was available for use at below 120°C. The rod position detector presented here, however, has been developed to be proof against the high temperature water with high accuracy even for temperature change. This non-contacting position detector contributes also to simpleness and compactness of the system.

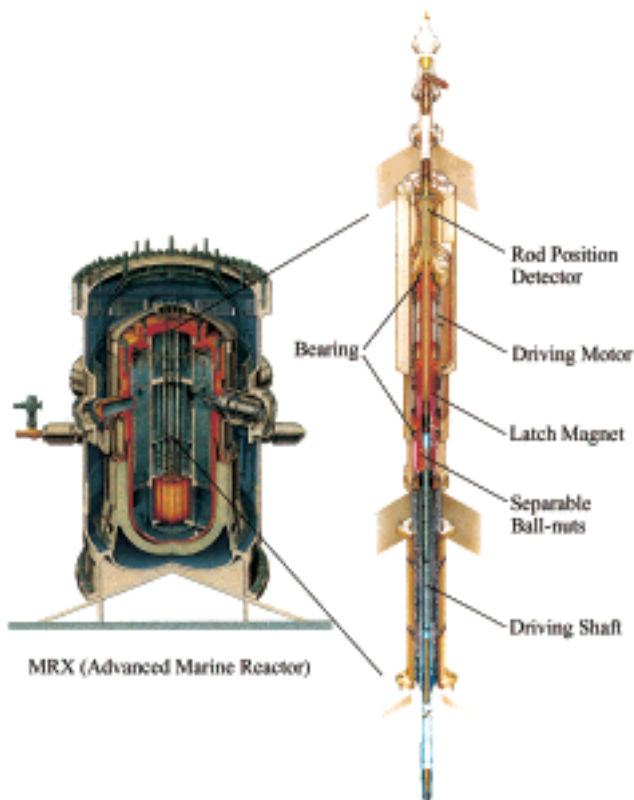


Fig. 1 Concept of INV-CRDM for MRX

As shown in Fig. 1, the driving motor and the latch mechanism have the center hole, where the driving shaft together with a magnet of the rod position detector moves vertically. This arrangement is also effective for compactness of the system. Cables for a rod position detector signal and electric lines of the motors penetrate the reactor pressure vessel.

Major parameters are given in Table 1 comparing with that of a typical PWR, which are of the out-vessel type CRDM. The outer diameter of the INV-CRDM of MRX is smaller than the other. The maximum required drawing force to the INV-CRDM of MRX is 2.2 kN, including vertical load of the CRDM, the total weight of control rod cluster, and a spring force (1.1 kN) helping scram at the condition of any ship posture within the limited time. Upon material, whole of the CRDM is made of inorganic materials, not organic material,

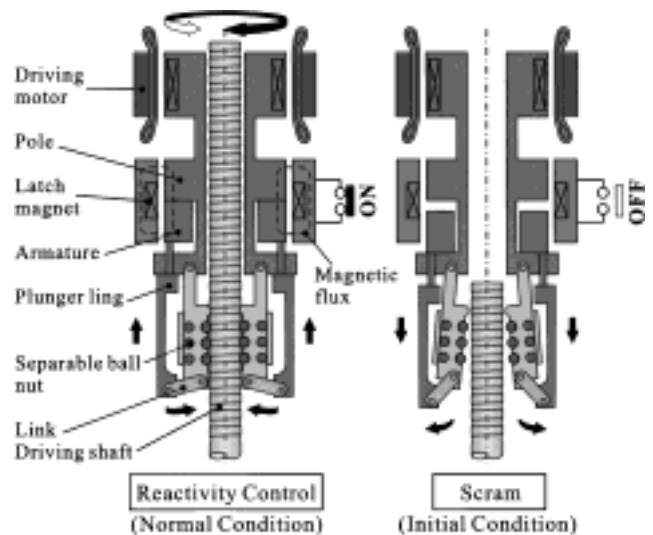


Fig. 2 Motion of latch mechanism

taking account of operating condition under high temperature water and the radioactive rays. De-tails of the design of main components are described in the following.

2. Design of Driving Motor

A cross sectional view of the driving motor is shown in Fig. 3. The motor consists of the rotor and the stator. The rotor has 8 poles made of Sm₂-Co₁₇ type magnet, which are fixed to magnet yoke and covered by a thin case made of Inconel for waterproof. The Sm₂-Co₁₇ type magnet was selected because of excellent features: It exhibits the highest heat and corrosion resistance among high performance rare-earth magnets.⁶⁾ It has a high Curie temperature, 750°C, and a high remanent flux and a small irreversible flux loss of the magnet at high temperature.

The demagnetization curve of magnet at elevated temperatures were measured⁷⁾ for development of the INV-CRDM by specimens machined from pieces of sintered Sm(Co_{0.61}, Fe_{0.28}, Cu_{0.08}, Ni_{0.01}, Zr_{0.02})_{7.3} magnets. The demagnetization curve obtained is shown in Fig. 4. Coercive forces of the magnets decreased with the elevated temperature. In design of the driving motor, the load lines of the magnets crossed the liner part of B-H curve at temperatures below 623 K, imply-

Table 1 Major parameters of INV-CRDM and comparison with conventional one

Item	MRX	PWR
Type	In-vessel, motor driven	Out-vessel, Mag-jack
Operating condition	In the primary water (310°C, 12 MPa)	Magnet coil in air (<180°C, 0.1 MPa)
Dimensions		
Outer diameter (mm)	200	274
Total length (mm)	1,735	4,468
Stroke (mm)	1,400	3,620
Drive force required	2.2 kN for drawing up	About 1.6 kN for drawing up
Scramming force by	Weight and spring	Weight
Design operational life	20 years	40 years

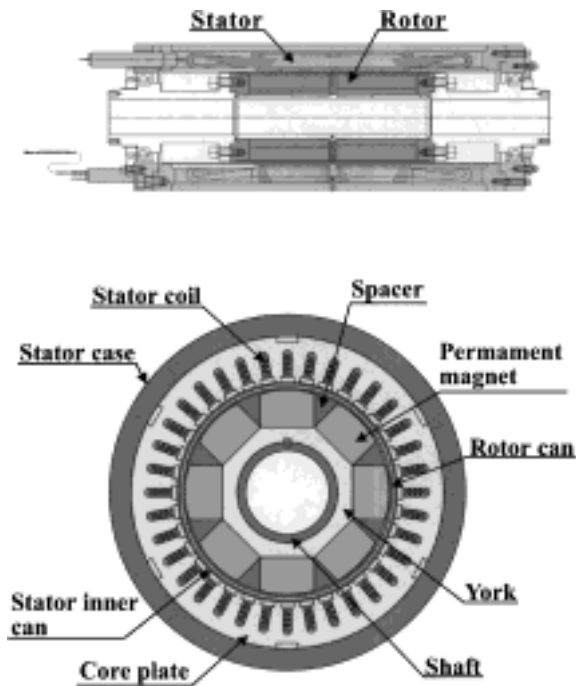


Fig. 3 Cross sectional view of driving motor

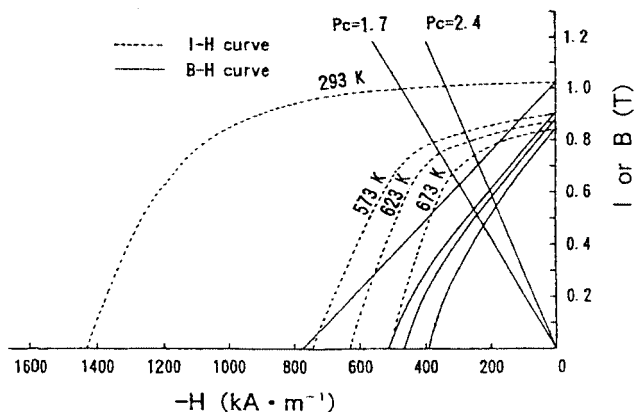


Fig. 4 Demagnetization curve of $\text{Sm}_2\text{-Co}_{17}$ magnet, by Iida *et al.*⁶⁾

ing that the irreversible flux loss of the magnets is small in the actual working condition (573–603 K).

Long-term stabilities of the $\text{Sm}(\text{Co}_{0.61}, \text{Fe}_{0.28}, \text{Cu}_{0.08}, \text{Ni}_{0.01}, \text{Zr}_{0.02})_{7.3}$ magnets were also studied⁷⁾ with specimen of cylindrical shape with a diameter of 10 mm and varied lengths of 6.6, 8.8, and 12.3 mm. These length-to-diameter (L/D) ratios correspond to the permeance coefficient (P_c) of about 1.3, 1.7, and 2.4 respectively. The test was conducted at the temperature range of 300 to 360°C in an atmosphere filled with Ar gas. The test result presented in Fig. 5 shows that within 500 h, the normalized remanent flux sharply dropped in the all cases. This phenomenon is known as an initial demagnetization. After 500 h, it decreased gradually with the elapsed time and the demagnetization from 10,000 to 19,000 h were about 1–1.5% at 300°C, 1.5–2% at 330°C, and about 2% at 360°C respectively. Main reason for the gradual demagnetization was concluded as oxidation of magnet at a surface on

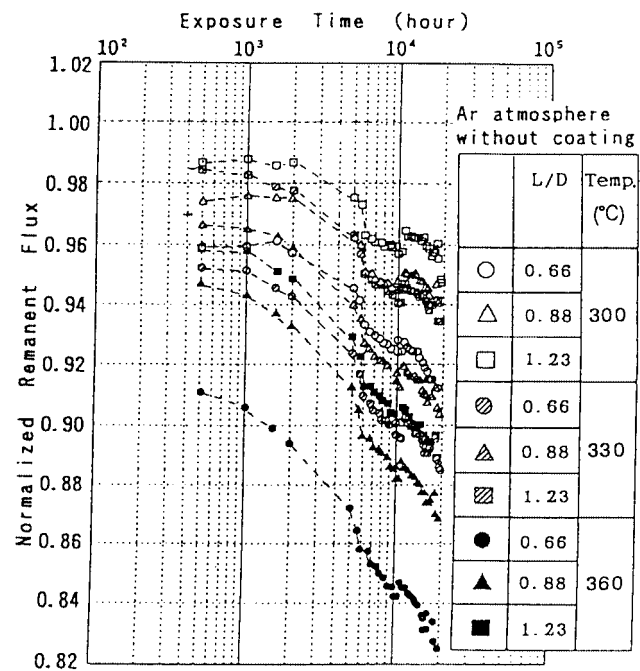


Fig. 5 Change in open-circuit remanent flux of $\text{Sm}_2\text{-Co}_{17}$ magnet during exposure, by Iida *et al.*⁶⁾

the base of measuring of the amount of oxide.⁷⁾

For the actual rotor, the magnets of 8 pieces are designed, which are covered by a can to prevent them from oxidation by water. The P_c value of the magnet will change in the range within about 0.68–1.23, demagnetizations of which were obtained by the specimen.

The stator is made of layered pure iron plates coated by ceramics for electrical insulation, providing 36 slots. In the slots, the mineral insulation (MI) coils are rested, the core of which is made of copper, insulated electrically by mineral material MgO , and coated by a non-magnetic material at the outer surface, the Inconel. The outer diameter of the coil is 2.4 mm. Though in the original design,⁴⁾ the coils were made of heat-resistant electric wire SHR-3 (compound of organic/inorganic insulated electric wire), the design was changed finally to adopt the present MI cable, taking into account of easiness and low cost of fabrication. The outside of stator is also covered by a thin can (or case) made of Inconel to avoid direct contact with the water. Since the Inconel is a non-magnetic material, there is a magnetical gap of 1.1 mm between the rotor and the stator, which is relatively large one comparing with a conventional motors. Due to this large gap, however, change of the load line in the B-H curve shown in Fig. 4 can be remained in a small range.

Major parameters are given in Table 2. The revolution speed of the driving motor is 50 rpm corresponding to one of the design conditions, the maximum linear movement speed 300 mm/m. The speed was changed from the original design 1,200 mm/m by evaluating with transient analyses of the MRX.¹⁾

The maximum required torque of the driving motor was calculated to 3Nm from the required drawing force 2.2 kN, the screw lead of the driving shaft 0.6 mm, and the total me-

Table 2 Major parameters of driving motor

Item	Parameters
Type	Synchronous motor
Rotor	
Magnet	8×2(row) pieces of Sm ₂ -Co ₁₇ type magnet 31 mm(breadth)×21.6 mm(height)×110 mm(length) with R59 mm(curvature)
Yoke	Pure iron
Can	Inconel, thickness of 1.5 mm
Inner diameter of the rotor	48 mm
Outer diameter of the rotor	121 mm
Stator	
Coil	MI cable(outer diameter=2.4 mm)
Structure for magnetic field	Pure iron coated by ceramics
Maximum available current	13.4 A
Inner diameter of the stator	124 mm
Outer diameter of the stator	200 mm
Can	Inconel, thickness of 1.5 mm
Revolution speed	50 rpm
Required motor torque	3Nm
Motor power at required power	54 W
Motor efficiency at required power	29%

chanical force transfer efficiency of the bearings and the ball screw of separable ball nut 0.7. A magnetic field analysis estimated that the three phase alternative current for the motor of 6 A were enough to produce this motor torque. The maximum allowable current for the coil was designed as 13.4 A from the limitation of heat removal of the coil.

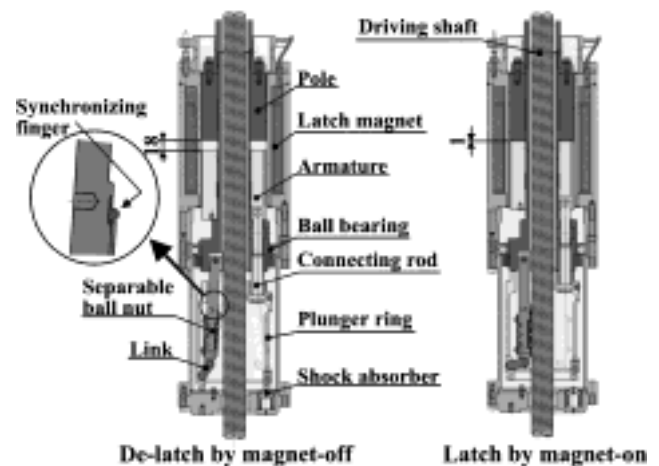
This synchronous motor is controlled by a sensor-less open-circuit control scheme,⁴⁾ which does not need any sensor to detect the position of magnetic field and enable the system being very simple, although sufficient currents for standing the maximum required torque should be supplied always to the stator coil even at the rest of rotor. Rotational speed of the rotor can be controlled by an inverter through change of a power angle frequency.

Upon dimension, the outer diameter of the stator is 200 mm. The cable support is arranged outside the stator, which is square with a side length of 205 mm. This size satisfies the design condition.

Performance of the driving motor such as the torque, controllability was verified by the test at the same condition as that of MRX, which will be described in the next chapter.

3. Latch Mechanism Design

Conceptual drawing of the latch mechanism is shown in Fig. 6. It contains an electric latch magnet, a pole, an armature, connecting rods, link rods and the separable ball nuts. The latch magnet consists of a casing, a coil bobbin and coils. The casing is made of the magnetic material SUS403 for magnetic path, the coil bobbin of the nonmagnetic material Inconel, and the coils of the MI cables. When the latch magnet is de-energized, the armature is apart from the pole at a distance of 18 mm. The ball nuts are also separated from the driving shaft as shown in Fig. 6. The magnet energized by a direct current pulls the armature to the pole with clearance of 1 mm remaining. This motion draws up the connecting rods

**Fig. 6** Cross sectional view of latch mechanism

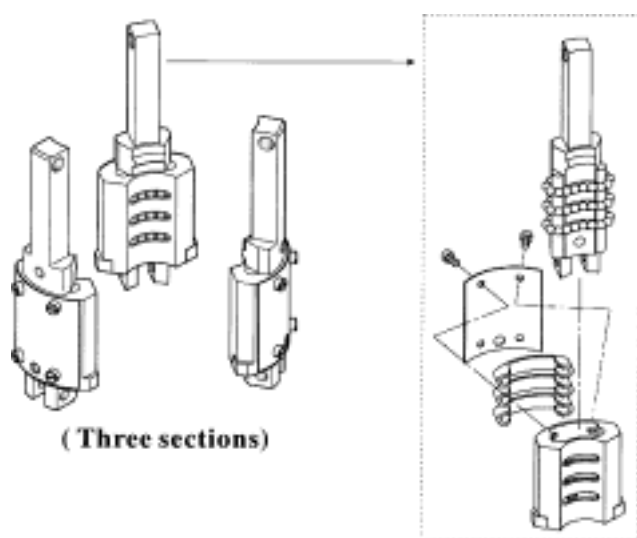
and the link rods, and the ball nuts grasp the driving shaft by a link device. De-energizing the magnet can make scam motion as mentioned before.

Parameters of the latch mechanism are presented in Table 3. The pulling force required for the magnet to lift the pole with the gap 18 mm was designed as 0.3 kN, and that to hold it with the gap of 1 mm as 0.6 kN, by accounting the weight of this mechanism and a partial force of the driving shaft's load. The minimum electric current of 7 A to lift and 1.5 A to hold were estimated by a magnetic field analysis.

The separable ball nut is a key device in the latch mechanism. This ball nut is divided into three sections as shown in Fig. 7 in order to be capable of latching and de-latching. Each section has three independent paths for balls, where balls circulate along by rotating. Mechanical issues of this ball nut device were how to hold the balls inside the path without dropping out, and the balls and the screw of driving shaft not to be

Table 3 Major parameters of latch mechanism

Item	Parameters
Type	Separable ball nut used type
Latch magnet	
Coil	MI cable (outer diameter of 2.4 mm)
Maximum current	13.4 A
Coil turns	400
Force to hold	0.6 kN
Force to latch	0.3 kN
Stroke of armature	17 mm=18 mm(de-latch)–1 mm(latch)
Separable ball nut	
Number of ball	18×3(stages)× 3(sections)
Diameter of ball	6.35 mm
Driving shaft	
Material	SUS 316 coated by cobalt alloy
Screw lead	6 mm

**Fig. 7** Separable ball nuts

hurt in latching motion.

On the first item, to hold the balls inside the path, a special cover case shown in the figure was designed and fabricating method was developed. Selection of material and fabrication technique of the ball nuts and the screw of shaft were especially important. These materials were the same ones as those of the ball bearing. A fine machining technique was finally applied for fabricating the ball nuts after try-and-error of fabrication.

Upon the second, if the balls hit the screw thread in latching motion, the balls and the screw will be damaged. To avoid this, a synchronizing finger has been devised and patented, which is a small projection with a half-circle profile mounted at upper part of the separable ball nut. The idea of device is that in the latch motion, these fingers touch the screw prior to mechanical ball touch and then the ball nut will be rotated along with the finger in a certain degree, and during the rotation, the finger can completely sit on the valley of the screw.

Function of the latch mechanism with a innovative technology was examined by the test at the room temperature and

then real operating condition, which will be described later.

4. Design of Ball Bearing

Two bearings are set in the INV-CRDM, the thrust and the radial bearings. The former should endure more severe load than that of the latter. That is, the load of the former is the sum of the weights of INV-CRDM components relevant to rotation and the control rods, and the spring force. The latter acts a role of anti-vibration measure in the rotational system. Both of the bearing types are the same, single row deep groove ball bearing.

Drawing and major parameters of the thrust bearing are shown in **Fig. 8** and **Table 4**, respectively. It consists of the balls, the races, and the retainer. Since an oil lubrication cannot be applied due to high temperature circumstance, the present bearings should bear a very severe tribo-field. Finding out of the applicable materials without oil lubrication for the bearing was required. A lot of screening tests were conducted with various combinations of the materials including metals, ceramics, alloys, and graphite. De-tails of the tests will be presented in other paper.

Result of the latest screening test with a small size test piece⁸⁾ is shown in **Fig. 9**. This result revealed that the retainer made of graphite has a very important role of not only holding the ball inside the inner and outer races, but also making an excellent tribo-field for the ball and the races, *i.e.*, an excellent lubricant. The materials given in the table are the ones selected from this test, taking account of easiness in fab-

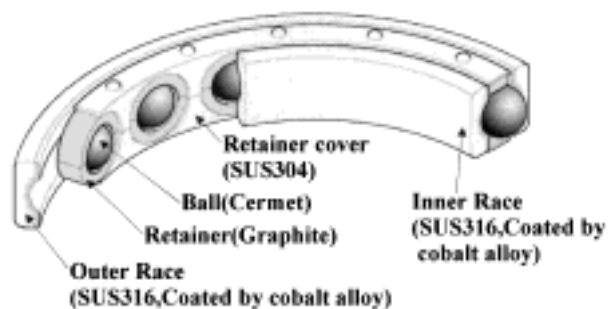
**Fig. 8** Cross sectional view of ball bearing

Table 4 Major parameters of the thrust ball bearing

Item	Parameters
Type	Single row deep groove, No. 6924
Axial load	2.2 kN
Revolution speed	50 rpm
Materials	
Outer and inner races	SUS 316 coated by cobalt alloy
Ball	Cermet
Retainer	Graphite
Dimensions	
Inner diameter	120 mm
Outer diameter	165 mm
Height	22 mm
Ball diameter	About 14.3 mm
Number of balls	17

rication.

Durability test of the ball bearing with the full sized one was conducted to confirm its availability for operation during the lifetime of INV-CRDM, described later. The target of rotation number to the ball bearing rotating around the shaft was derived as 1,160,000 from the total length of the driving shaft's stroke of the MRX in the 20 years operation on the base of the MUTSU experimental data. In the normal operation of the MRX reactor, movement of the control rod is considered to be required in entering and leaving a port, and maintaining the reactor power level according to the shipload at a rough sea condition. MUTSU experimental data on the control rod movement in these events were used for counting the total stroke of control rod. Detail of it will be published in a report from JAERI.

5. Rod Position Detector Design

The principle of the rod position detecting method using the magnetostrictive wire sensor is briefly presented referring Fig. 10. The rod position detector consists of a mag-

netostrictive wire, a magnet and a pulse unit for emitting an electric pulse and receiving a strain pulse. The magnetostrictive wire made of a strong magnetic material containing Fe and Ni will be strained by torsion force due to magnetic force during the electric current passes through, known as Wiedeman's effect. When the electric current pulse introduced from A point reaches the point, where the magnet placed, the torsional strain pulse will be emitted from this point and it will travel at the elastic wave speed u to the detector. The length l between the place of the detector as the base point and that of the magnet attached to the driven shaft can be calculated by elapse time Δt from the emitting electric current pulse to arrival of the strain pulse as $l = \Delta t \cdot u$, where the velocity of electric current is neglected.

Design of the position detector is shown in Fig. 11 and the major parameters in Table 5. The magnetostrictive wire is arranged inside the support tube covered with the well (or sheath) in the reactor vessel. The magnet is inserted into the head of driving shaft. The position detecting part is set outside the reactor vessel wall. Temperature change in the surrounding causes the signal error, since the velocity of the

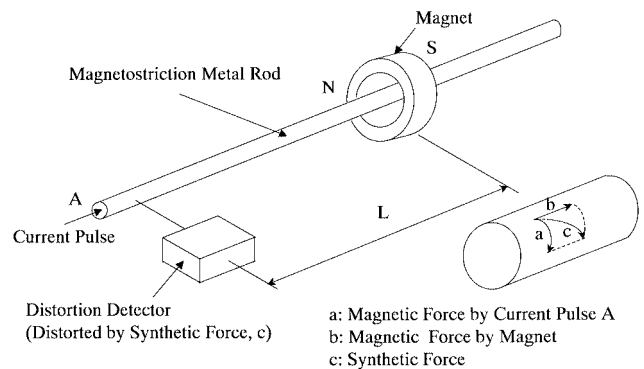


Fig. 10 Principle of rod position detecting method with magneto-strictive wire

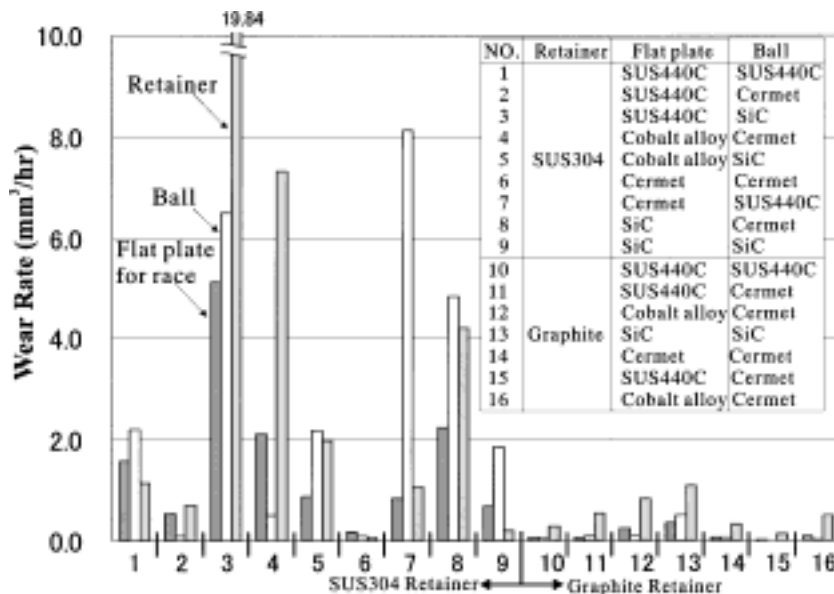


Fig. 9 Screening test result on the ball bearing

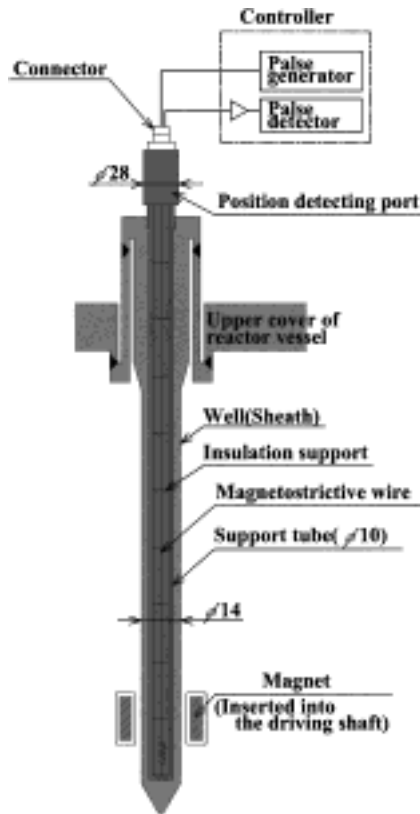


Fig. 11 Concept of rod position detector system

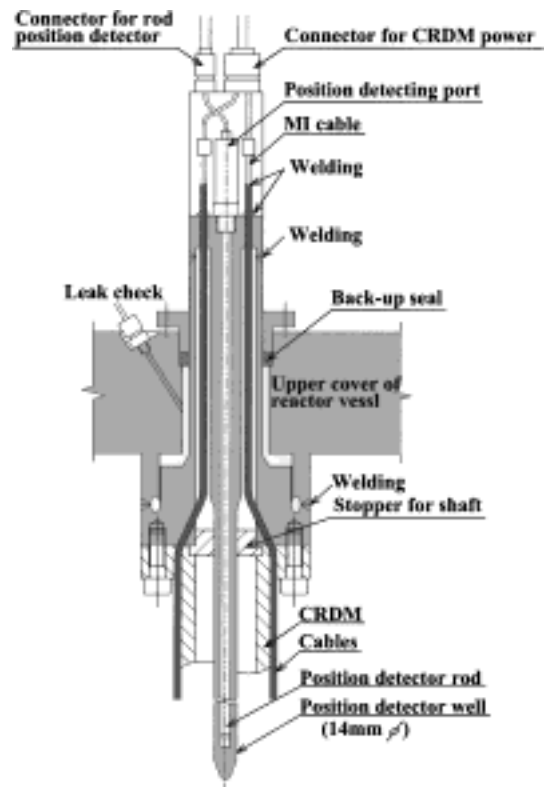


Fig. 12 Concept of cable penetration structure

Table 5 Major Parameters of the rod position detector

Item	Parameters
Type	Magnetostrictive wire with magnet
Working temperature	320°C
Actual detecting length	1,400 mm
Detecting error	±1.2 mm in 1,400 mm length
Dimensions	
Diameter	14 mm
Total length	2.4 m
Materials	
Wire	Ni-Fe
Magnet	Sm-Co type permanent magnet

strain pulse passing through the wire is easily affected by temperature change. This change can be adjusted with a compensation circuit by detecting change of the electric resistance due to temperature change. Accuracy of this position detector has been certified by a test to be within 1.2 mm of the error in this configuration at the temperature of 310°C—the error was confirmed to be within 0.5 mm.

6. Cable Penetration Structure

As the whole of CRDM is installed inside the reactor vessel, a cable penetration for the electricity and the signal through the wall is provided. A concept of the cable penetration structure is shown in Fig. 12. The penetrating cables consist of three for the driving motor and two for the latch magnet. The rod position detector tube covered with the well

(or sheath) also penetrates the wall. The MI cable are connected to the connectors outside the wall. Seals by welding are made at both of the outside and the inside of the reactor vessel wall. Leakage from the seals can be easily detected by leak check shown in Fig. 12.

It is also very important in practice to be capable of inspecting or repairing easily the INV-CRDM at the chance of refueling or the In-Service Inspection (ISI) of the reactor plant. A procedure or method of the inspection of the present INV-CRDM is basically the same as that of the conventional PWRs. Outline of the procedure of the inspection and repairing will be described in the **Appendix**.

IV. Functional Performance Test

Each component mentioned above was separately tested with a small scale or full sized ones on their performance at conditions of the room temperature or the high temperature. Following the tests of each component, the full sized components were assembled for an overall performance test and endurable test at the same condition as the MRX operation. The purpose of the tests was to confirm that it covers the required functions mentioned in the design condition.

1. Test Assembly

The test section consisting of the driving motor, the latch mechanism, the ball bearing and the driving shaft was installed in the pressure vessel as shown in Fig. 13. Water pressurized to 12 MPa by a pump was fed into the vessel, and it became high temperature water of 310°C by a heater set outside the pressure vessel. At the upper space of the test section,

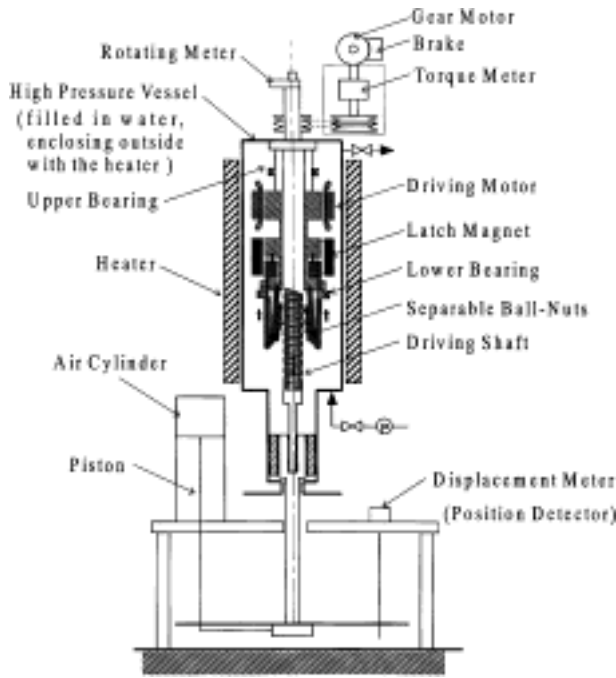


Fig. 13 Test assembly for functional performance test

the revolution speed meter, the torque meter, and the geared-motor with the brake for measuring the torques of the driving motor or whole the load with the driving motor freed were arranged. Toque of the driving shaft was transmitted to the torque meter through a magnet coupling.

At the lower space of the test section, an air cylinder system was placed to adjust the vertical load acting on the shaft. In the test assembly, the spring coil was not used and the driving shaft was shorter than the full size, for convenience. All components except the spring coil and the shorter driving shaft, were full sized ones. The rod position detector was attached to the rod connected with the driving shaft.

The control system with inverters controlled the electric currents for the heater, the driving motor, the geared motor and the latch magnet. The data logger recorded the data of the revolution speed, the torque, the electric current, the pressure and the temperature of the water, and the rod position.

2. General Behavior

Typical operation of the driving shaft's upward and downward movement, holding the same position, and the scram is shown in Fig. 14. It started firstly by latch motion. The driving shaft was grasped by the separate ball nuts by energizing the latch magnet. It was found that the rotation of separable ball nut in one round, 360 degrees peripherally was necessary for complete latch motion by the synchronizing finger. For latch motion, therefore, the driving motor rotated always in only one revolution.

After completion of latching motion, the driving shaft was repeatedly drawn up and down by the driving motor. Finally, the latch magnet was de-energized by cutting the current for scram. As the general performance tests, the similar pattern as shown in Fig. 14 was repeated. From the test it was confirmed that the driving shaft can be moved accurately, stably

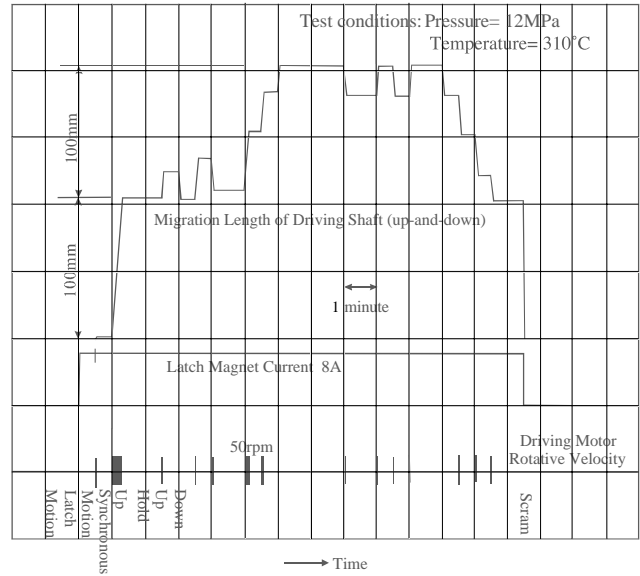


Fig. 14 Typical operation of functional performance test

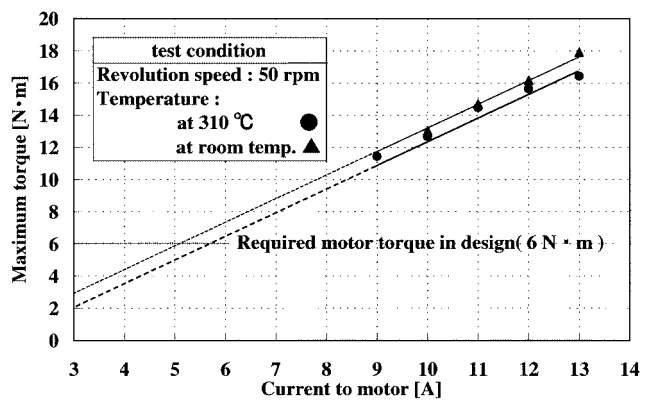


Fig. 15 Measured maximum torque of the driving motor

and calmly following to an arbitrary order through the control system.

3. Driving Motor Performance

The maximum torque of the motor T_{max} , over which it can not synchronize, depends on the current and the operating temperature. The values of T_{max} were obtained from a loading torque T_l , a resistance torque of the motor itself when it was forced to rotated by the geared motor T_r , and a braking torque T_b ; $T_{max}=T_l+T_b-T_r$. The loading torque T_l , was measured by using the geared-motor and by de-energizing the driving motor. The resistance torque T_r was estimated by a magnetic field analysis. The braking torque T_b , which includes the friction torques of the rotating ball bearings, the magnet coupling, the sealing, etc., was measured using the driving motor and the brake.

The measured T_{max} is shown in Fig. 15 for various currents at the elevated temperature and the room temperature, and at the revolution speed of 50rpm. The values of T_{max} increased with the current. The values of T_{max} at the elevated temperature were slightly smaller than those at the room temperature.

This decrease was mainly due to reduction in the magnetic flux density of permanent magnet at high temperature. Design value of current 6A was confirmed by this test to have a reserve against about 3.5 A equivalent to the required torque of the motor in the normal operation, mentioned in Sec. III-2.

After functional test of the driving motor, it was overhauled. Any crack or scratch was not detected on the cans covering the rotor magnets and the stator, that is, intactness of them against the high temperature and pressure water was verified. The functional performance test revealed that the driving motor was capable of supplying the required torque at the severe condition, as expected.

The normalized remanent flux of permanent magnets was measured by comparing the remanent fluxes of virgin magnets and those of magnets exposed in the atmosphere of elevated temperature 310°C for an accumulated period of 200 h. Reduction of average remanent fluxes was about 4%, which was considered as the initial demagnetization. This demagnetization value was close to the data for the P_c of 1.3 or the L/D of 0.66 shown in Fig. 5, and it was slightly greater than the result of the long-term stability test. The reason is considered as that the reverse magnetic field due to electric interaction between the coil and the magnet at the functional test was greater than that of the design because the current to motor was relatively large, so that an irreversible flux loss of the magnets occurred during the test.

Since the magnets were covered with the can, demagnetization due to oxidation would not occur in the real operation as long as the can is intact. The reduction of remanent flux during the operating life, therefore, can be said about 5% at most and its effect on the driving motor torque can be negligible.

4. Latch Mechanism Performance

To survey function of the latch mechanism, the minimum currents for the latch magnet to latch or to hold the driving shaft, and the de-latch time were measured. The minimum currents, below which the separable ball nuts cannot grasp the driving shaft, was obtained by decreasing the current until onset of de-latching. The de-latch time was measured with the test parameters of the current to the latch magnet, and the operating temperature.

The minimum current in latch motion was about 7.1 A at the temperature of 310°C and also at the room temperature, which was almost the same as that of design value. The minimum current to hold the driving shaft after latch motion was 1.6 A at the temperature of 310°C, while 1.1 A at the room temperature. These were almost the same as the design one. The slight increase of the minimum current at the elevated temperature were considered due to decrease of the magnet force according to temperature rise.

In the performance test shown in Fig. 14, the current to the latch magnet was held at a constant of 8 A despite of any motion, although the minimum current for the latch magnets depends on the motion. Since the current of 8 A, however, is too large for holding, it should be changed according to the motions. This is necessary especially for a long period operation, but it can be easily done by using a control system to change the current to the magnet.

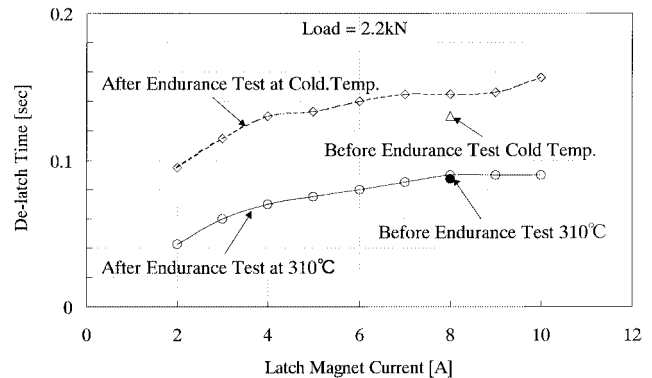


Fig. 16 Measured de-latch time

In measurement of de-latch time, the initial current to the magnet ranged from 2 A to 10 A. The vertical downward force of 2.2 kN was loaded on the driving shaft, which is the same as the load of the MRX. The de-latch times measured are shown in Fig. 16. They increased with initial currents to latch magnet, that is, magnetic force. For all currents, the de-latch times were verified to be smaller than the design value. The de-latch time at the high temperature were shown to be shorter than those at the room temperature. Main reason of this difference is considered due to the difference of the flow resistance of fluid. In de-latch motion, water should flow into the space between the armature and the pole passing through a narrow flow path. The flow resistance differs by the fluid temperature. Ratio of the kinetic viscosity of water at the high temperature 310°C to that of the room temperature is about two, which is almost the same as that of the de-latch time.

According to the design conditions for repeating scrambling, the de-latching motion was repeated in 1,000 times, and the de-latch times measured at the beginning and at the last time, as shown in the figure. There were few differences between the both, which were within a range of measuring error. As a result, the de-latch times were found to be smaller than that of design value, 0.2 s.

5. Ball Bearing Durability Test

The durability test of the ball bearing was conducted by rotating the shaft at the condition; the rotation speed of 50 rpm, the temperature and pressure of water, 310°C, 12 MPa, respectively. In this test, the driving motor, the latch-mechanism and the air cylinder system were removed from the test assembly, in turn the weight to compensate the total load was attached. The shaft was rotated with the geared motor. The torque of the shaft were measured during the rotation.

The torque is shown in Fig. 17 against a accumulated revolution number of the ball bearing. The torque increased gradually with revolution. While the torque remained at a low level for below about 1,200,000 revolutions, it increased sharply for over 1,200,000, and an abnormal noise due to vibration of the test assembly was detected by using a stethoscope rod. Since it seemed a limit to continue rotation, the test was stopped, at the total revolution of 1,250,000. As a result, it can be said that the ball bearing held the integrity up to

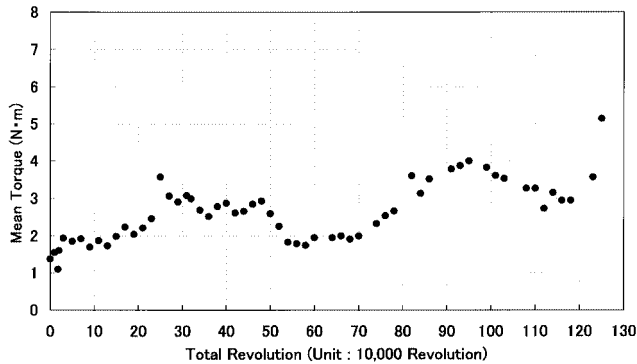
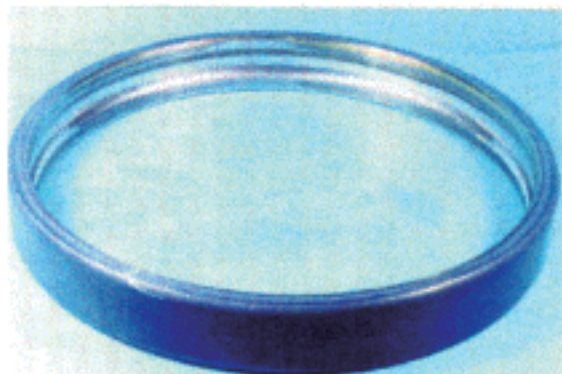


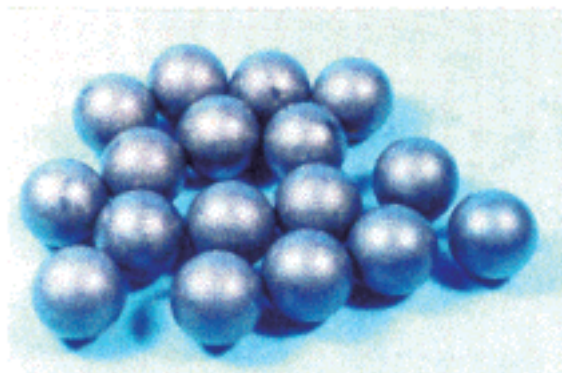
Fig. 17 Result of ball bearing endurance test



Inner race



Outer race



Ball

Fig. 18 Overhauled thrust ball bearing after endurance test

1,200,000 revolutions, that is, the design target of 1,160,000 was attained.

Mechanism of sharp increases of the torque and vibration after this revolution in the test is considered as follows. The support rigidity of the rotational system containing the ball bearing decreased due to wear of the ball bearing. The first mode critical revolution speed of the system also decreased and it had a chance to coincide with the operational revolution speed somewhere after the revolution exceeded 1,200,000. Resonance caused the sharp increases in both the vibration and the torque.

The balls, the retainers and the races were examined by dismantling after the test. There was not any crack on them except of a small chipping at a shoulder of the retainer of the thrust ball bearing. Wears of the radial ball bearing was less than those of the thrust ball bearing. Photograph of these components of the lower ball bearing is shown in Fig. 18. All the balls wore out in depth of 23–31 μm . Wears of the inner race and the outer race were 140 μm and 60 μm , respectively. Since the surface contact pressure of the inner race during rotation is in general greater than that of the outer race, the wear of the former is greater than that of the latter. The retainer showed the wear of about 1 mm at every pocket.

V. Discussions on Satisfaction of Design Condition

1. Compactness

The cross-sectional size of the INV-CRDM does not exceed the design condition of 205 mm in square by using effectively the center hole of the motor for stroke of the driving shaft and the rod position detector. However, the latch mechanism adopting the separable ball nuts will restrict furthermore compactness than the present sized-one. That is, when more compactness of the INV-CRDM is required for a very small reactor, the same type of the latch mechanism will not be applied.

On the total length, it has a reserve for the design condition with the stroke of 1.4 m. On the other hand, even if longer stroke is required *e.g.*, for a reactor with greater power, this design concept can be applied without change.

2. Driving Function

The performance test proved that the latch mechanism was able to latch or hold stably and smoothly the driving shaft, and the driving motor to provide enough torque to rotate the shaft at the required speed under the condition of high temperature and pressure water.

The driving motor was confirmed by the test to be capable of maintaining the enough power for a long time operation—the effect of demagnetization of the permanent magnet due to oxidation can be decreased greatly by the covering case of it. On the other hand, increase of the load due to worsening of mechanical efficiencies of the ball bearing or the ball nuts for a long time operation should be taken into account. Provided that the total mechanical transfer efficiency reduces to a half of the initial one, 0.45, the required motor torque will become twice of the design value. Even for this case, it is within the maximum motor torque T_{max} for the motor current of 6 A. The value of T_{max} , however, can be changed easily by the motor

current up to 13.4 A.

Accuracy of adjusting the control rod position of the present INV-CRDM depends on that of the rod position detector and a non-controlled area of the driving motor having 8 poles in its rotation. However, errors in adjusting the rod position due to both can be estimated as 2 mm at most—error of the former is 1.2 mm as shown in Table 5, and that of latter is 0.8 mm.

Apart from the marine reactor, in application to the land-based reactors, the operating condition for the CRDM will be milder, since the spring force for an abnormal ship posture is not required, and the motor torque can be smaller.

3. Scramming Time and Scram under Ship Posture

For the normal ship posture, it was verified by the test that the de-latch time in the scramming was below the design value 0.2 s for the operating conditions of high temperature and room temperature, and the currents to the latch magnet.

For the various ship posture, the de-latch time was measured by inclining the test facility at the required inclination attitude up to 180°—being overturned. The test, not described in the presented paper, was conducted at a room temperature. The de-latch times were within 0.2 s for the inclination up to 60 degrees. It was about 0.2 s at 90 degrees inclination. Once de-latch is done, scramming will be completed by a strong downward force of the spring, which was designed by taking account of the various direction of the gravity force.

4. Circumstance for INV-CRDM Working

It was verified by the test that the present INV-CRDM could operate in the high pressure and temperature water. The effect of radioactive rays on the material is discussed as follows.

The intensities of γ -ray and neutron at the place for the INV-CRDM of the MRX were obtained from a design analysis on the radiation shielding. With the analysis, the total radiation fluxes for 20 years were estimate as $3 \times 10^{10} \text{ cm}^{-2}$ by γ -ray, and $3 \times 10^3 \text{ cm}^{-2}$ by the epi-thermal neutron (0.1 eV–1 MeV) and $3 \times 10^2 \text{ cm}^{-2}$ by the thermal neutron (<0.1 eV). Dose equivalent rates of the total γ -ray was $9 \times 10^{-1} \text{ Sv}$, and that of the total neutron $9 \times 10^{-8} \text{ Sv}$. Irradiation by γ -ray was found to be dominant. It, however, did not contain radiation from an irradiated crud. The dose equivalent rates of γ -ray by a crud for 20 years was estimated as about $5 \times 10^4 \text{ Sv}$ on the base of existing PWR's data.

Materials influenced by irradiation are considered as the insulation, MgO, of MI cable and the permanent magnet, Sm₂–Co₁₇ type magnet, of the driving motor. The MgO was affected by neutron irradiation on the insulation performance, reported by Nakamichi *et al.*⁹⁾ However, since the reported neutron flux, 10^{19} cm^{-2} , was subjected on a fusion reactor, it is far higher than that of the present case. Considering the fact that the thermo-meter using this material are adopted in the PWRs, the effect of it can be neglected.

Effects of γ -ray irradiation and neutron flux on the magnetic flux of the permanent magnet were experimentally surveyed by researchers. The γ -ray irradiation of $2.8 \times 10^6 \text{ Sv}$ using Co decreased the magnetic flux by 0.5%, reported by Okuda *et al.*¹⁰⁾ The neutron irradiation of $2.6 \times 10^{18} \text{ cm}^{-2}$

caused reduction of the magnetic flux of 0.2%, reported by Cost *et al.*¹¹⁾

These data can lead that the effect of radioactive rays on the material in the present INV-CRDM for MRX is very small. Therefore, it does not need any special measure for irradiation of the materials.

5. Life Time

As described above, the driving motor and the latch mechanism are revealed to have the potential of working for a long period. The repeated number of de-latching on scram of 1,000 times was certified by the test. Integrity of the ball bearing under the severe condition is crucial for the period of the INV-CRDM life.

Durability of the ball bearing is determined by rolling wear, which depends on the load weighting on it, the rotation speed and the water temperature besides the materials. Since the heavier weight, the higher rotation speed and the higher temperature water, in general, induce the larger wear of ball bearing, the strong spring of MRX's INV-CRDM gives disadvantage on wear. Under the same condition as that of MRX operation, durability of the present ball bearing was verified by the test as 1,200,000 revolutions, covering the design target. Since the durability test of the ball bearing was conducted in only one time in the present study, repeating of the test would be generally desirable for confirmation of durability.

The ball bearing durability test, however, was conducted under two rather conservative conditions comparing with the MRX's INV-CRDM. One was that in the test, the lower part of the shaft was not supported *i.e.*, free. The other was that in the test the cylindrical weight for adjusting the load was attached, and the water-filled space between the weight and the pressure wall was narrow and vertically long. The water in this space can increase a virtual water mass in rotation of the cylindrical weight. These were considered to cause the reduction of the critical revolution speed of the system, and it was confirmed by an elastic rotation analysis. Unless there are these effects in the system, occurrence of resonance due to wear will delay. A longer life of the ball bearing, therefore, can be expected in real operation of MRX.

As a result, it can be said that the INV-CRDM of MRX is capable of working for the designed life period.

VI. Conclusion

A compact control rod drive mechanism to be installed inside the reactor vessel of the advanced marine reactor MRX has been developed. With performance tests under the high-temperature and high-pressure water, it can be concluded as follows.

- (1) The position of control rod can be controlled stably, smoothly and accurately. The driving shaft can move by a speed of 0–300 mm/m.
- (2) For scram, de-latching can be completed within 0.2 s even at inclined attitude up to 60 degrees. The inclined attitude corresponds to a ship posture.
- (3) Damage of the components by irradiation of γ -ray and neutron is estimated to be negligibly small.
- (4) For the operational period of the INV-CRDM, integrity

of the ball bearing is crucial. It is clarified that operation period of the INV-CRDM over 20 years is available.

The developed INV-CRDM can be adopted not only for the MRX, but also for light water reactors, PWR or BWR. The technologies will be applied to the CRDM of a fast breeder reactor or a robot working at a severe condition.

Acknowledgments

The authors wish to express their deep appreciations to Dr. H. Iida of Japan Atomic Energy Research Institute (JAERI), K. Sako who retired from JAERI, and Y. Kasahara of Mitsubishi Heavy Industries, Ltd. for help of this works. The authors also appreciate co-operation of Mr. K. Hayashida of Koyo Co., Ltd., Dr. M. Kawamura of Mitsubishi Electric Corporation, and Dr. K. Morimoto of Mitsubishi Materials Corporation.

References

- 1) T. Kusunoki, *et al.*, "Design of advanced integral-type marine reactor, MRX," *Nucl. Eng. Des.*, **201**, 155–175 (2000).
- 2) Y. Wu, *et al.*, "Hydraulic control rod drive system for 5MW nuclear heating reactor," *J. Tsinghua Univ.*, **30**[6], 29 (1990).
- 3) H. Bo, *et al.*, "Step dynamic process of the hydraulically-driven control rod, (I); Experiment of dynamic process behavior," *J. Nucl. Sci. Technol.*, **37**[12], 1032 (1000).
- 4) Y. Ishizaka, *et al.*, "Development of a built-in type control rod drive mechanism (CRDM) for advanced marine reactor X (MRX)," *Proc. ANP'92: Int. Conf. on Design and Safety of Ad-*

vanced Nuclear Power Plants, Tokyo, p. 461–467 (1992).

- 5) D. V. Malyugin, "On the theory of Wiedeman effects," *J. Magn. Mater.*, **97**, 193–197 (1991).
- 6) W. Ervens, "Some properties of high-coercivity 2 : 17 magnets," *Proc. 6th Int. Workshop on Rare-Earth Cobalt Magnets*, Baden, p. 319–327 (1982).
- 7) H. Iida, *et al.*, "Long-term stability of $\text{Sm}_2\text{Co}_{17}$ -type magnets for control rod drive mechanism (CRDM) in a nuclear reactor," *IEEE Trans. Magn.*, **31**[6], p. 3653–3655 (1995).
- 8) I. Toshihisa, *et al.*, "Tribological characteristics of rolling bearings in high-temperature (320°C), high-pressure (11.8 MPa) water," *Proc. Int. Tribology Conf.*, Nagasaki, Oct. 29–Nov. 2, 2000, (2000).
- 9) M. Nakamichi, *et al.*, "Electrical properties on mineral insulated cables under neutron irradiation," *Proc. 20th Symp. on Fusin Technology*, Marseille, Sep., 1998, (1998).
- 10) S. Okuda, *et al.*, "Effects of electron-beam and γ ray irradiation on the magnetic flux of Nd–Fe–B and Sm–Co permanent magnets," *Nucl. Instrum. Methods Phys. Res.*, **B94**, 227–230 (1994).
- 11) J. R. Cost, *et al.*, "Radiation effects in rare-earth permanent magnets," *Proc. Material Research Symp.*, Materials Research Soc., Vol. 96, (1987).

Appendix

Procedure of Inspection or Repair of INV-CRDM

Since the whole of INV-CRDMs are installed inside the reactor vessel and are submerged in the primary water, radiation by irradiated crud's attached to the surface of components of

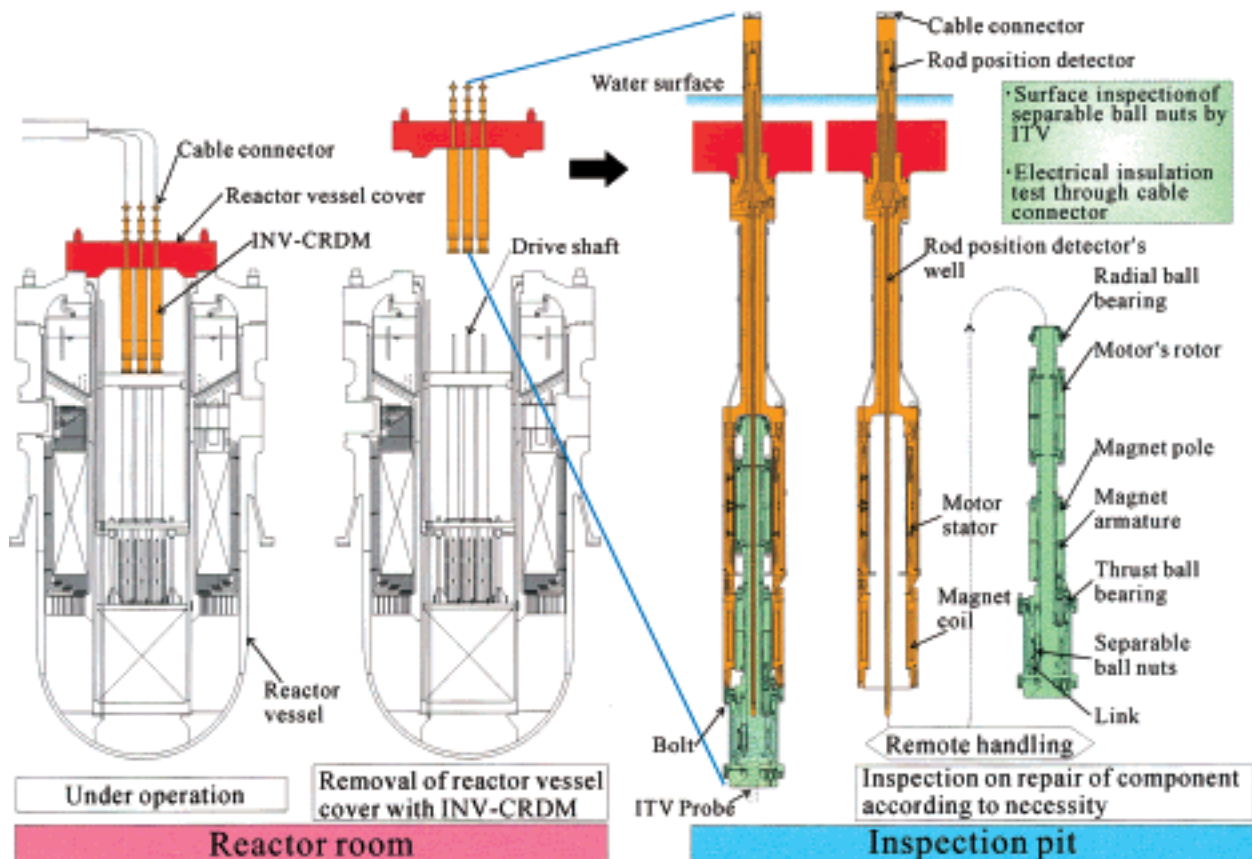


Fig. A1 Procedure of inspection or repair

INV-CRDM should be taken into account in the event of inspection or repair.

In refueling to be scheduled at every four years for the MRX, the reactor vessel cover together with the INV-CRDMs is removed after the all-driving shafts are disconnected from the INV-CRDMs by de-latching. This procedure is the same as that of the conventional PWRs. Outline of the procedure of inspection or repair is shown in **Fig. A1**.

By flushing the surface of the components with fresh water, the irradiated crud can be mostly removed. After flushing, however, the INV-CRDMs are transferred to an exclusive inspection pit, which is filled with water, in order to reduce the radiation exposure as possible as.

Some numbers of the INV-CRDMs, but not the all, are inspected by remote handling. Surface inspection with the ITV

is made on the overall surface, the outlooks of the latch mechanism and the separable ball nuts. Electrical non-conductance of the cables is tested through cable connectors, which are set outside the water surface.

Although it is not necessary as the periodical tests on the occasion of refueling to inspect the motor, the ball bearing and the latch magnet, if necessary, they can be inspected after dismantling by unfastening the bolts shown in the figure. When a defect happens to be detected, the component will be replaced with a spare one. For these handlings, an exclusive device, which will be fabricated without difficulty, needs.

Functional tests of the INV-CRDM on performance such as moving upward and downward, latching and scrambling are performed after resetting them inside the reactor vessel.